JACS
JOURNAL OF THE AMERICAN CHEMICAL SOCIETY
ARTICLE
pubs.acs.org/JACS

$[Ni(P^{Ph}{}_2N^{C6H4X}{}_2)_2]^{2+}$ Complexes as Electrocatalysts for H_2 Production: Effect of Substituents, Acids, and Water on Catalytic Rates

Uriah J. Kilgore,[†] John A. S. Roberts,*[,†] Douglas H. Pool,[†] Aaron M. Appel,[†] Michael P. Stewart,[†] M. Rakowski DuBois,[†] William G. Dougherty,[‡] W. Scott Kassel,[‡] R. Morris Bullock,[†] and Daniel L. DuBois*[,†]

[†]Center for Molecular Electrocatalysis, Chemical and Materials Sciences Division, Pacific Northwest National Laboratory, P.O. Box 999, K2-57, Richland, Washington 99352, United States

[‡]Department of Chemistry, Villanova University, Villanova, Pennsylvania 19085, United States

Supporting Information

ABSTRACT: A series of mononuclear nickel(II) bis(diphosphine) complexes $[Ni(P^{Ph}{}_2N^{C6H4X}{}_2)_2](BF_4)_2$ ($P^{Ph}{}_2N^{C6H4X}{}_2$ = 1,5-di(*para*-X-phenyl)-3,7-diphenyl-1,5-diaza-3,7-diphosphacyclooctane; X = OMe, Me, $CH_2P(O)(OEt)_2$, Br, and CF_3) have been synthesized and characterized. X-ray diffraction studies reveal that $[Ni(P^{Ph}{}_2N^{C6H4Me}{}_2)_2](BF_4)_2$ and $[Ni(P^{Ph}{}_2N^{C6H4OMe}{}_2)_2](BF_4)_2$ are tetracoordinate with distorted square planar geometries. The Ni(II/I) and Ni(I/0) redox couples of each complex are electrochemically reversible in acetonitrile with potentials that are increasingly cathodic as the electron-donating character of X is increased. Each of these complexes is an efficient electrocatalyst for hydrogen production at the potential of the Ni(II/I) couple. The catalytic rates generally increase as the electron-donating character of X is decreased, and this electronic effect results in the favorable but unusual situation of obtaining higher catalytic rates as overpotentials are decreased. Catalytic studies using acids with a range of pK_a values reveal that turnover frequencies do not correlate with substrate acid pK_a values but are highly dependent on the acid structure, with this effect being related to substrate size. Addition of water is shown to dramatically increase catalytic rates for all catalysts. With $[Ni(P^{Ph}{}_2N^{C6H4CH2P(O)(OEt)2}{}_2)_2](BF_4)_2$ using $[(DMF)H]^+OTf^-$ as the acid and with added water, a turnover frequency of 1850 s^{-1} was obtained.

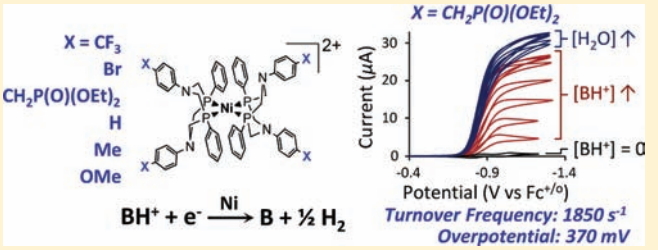

INTRODUCTION

Controlling the intra- and intermolecular movement of protons is an essential feature of catalytic processes involving multiple protons and electrons. For example, hydrogenase and cytochrome c oxidase enzymes have proton channels consisting of multiple proton relays that facilitate the exchange of protons between the catalyst active site buried deep within the protein matrix and the surrounding medium.[1,2] These proton channels deliver or remove protons precisely to and from the correct atom(s) of the active site. In the active site cluster of the [FeFe] hydrogenase enzyme, the nitrogen base in an azadithiolate ligand is proposed to mediate proton transfer to or from a coordination site at the distal iron atom, as shown in structure **1**.[3]

Several research groups have developed and studied synthetic complexes that incorporate bases in the second coordination sphere.[4] In our laboratory we have prepared nickel bis(diphosphine) complexes of the type shown in structure **2** and have probed the roles that the pendant bases play in the catalysis of multiproton and multielectron reactions.[5,6] Our studies have demonstrated that bases in the second coordination sphere function as proton relays, dramatically accelerating the rates of intra- and intermolecular proton transfer.[7−9] In addition, the pendant bases also stabilize the binding of small molecules, such as H_2 and CO,[9−11] facilitate proton-coupled electron transfers,[7,8]

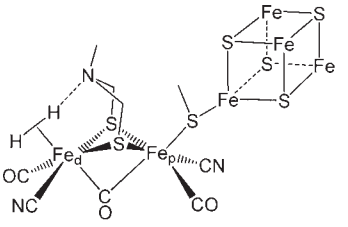

1

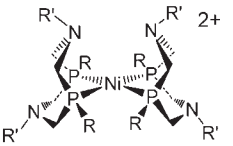

2

and lower the barrier for heterolytic cleavage or formation of the H−H bond.[7−15] These features contribute to the activity observed for $[Ni(P^R{}_2N^{R'}{}_2)_2]^{2+}$ complexes, **2**, for electrocatalytic H_2 oxidation and production[7−15] and for O_2 reduction.[16]

We have previously reported that $[Ni(P^{Ph}{}_2N^{Ph}{}_2)_2](BF_4)_2$ is an electrocatalyst for H_2 production, with a turnover frequency of 350 s^{-1} and an overpotential of approximately 300 mV using a solution containing protonated dimethylformamide ($[(DMF)H]^+OTf^-$) in a 1:1 molar ratio with DMF as the substrate in acetonitrile.[12] Under similar conditions the related complex $[Ni(P^{Ph}{}_2N^{Bz}{}_2)_2](BF_4)_2$ (Bz = benzyl) shows a turnover frequency for H_2 production of only 5 s^{-1}.[17] These results clearly indicate that

Received: October 29, 2010
Published: March 25, 2011

the nitrogen substituents of the $P^{R}{}_2N^{R'}{}_2$ ligands play an important role in the catalytic activity for these complexes and suggest that more basic amines disfavor catalytic H_2 formation. In this study we have prepared a series of $[Ni(P^{Ph}{}_2N^{C6H4X}{}_2)_2](BF_4)_2$ derivatives, in which the substituent X in the para position of the N aryl substituent is varied. Such substituent changes are expected to influence the basicity of the pendant amine while minimizing steric and electronic variations at the metal ion. We report here the effect of these substituent variations on the redox potentials of the Ni(II/I) and Ni(I/0) couples of the complexes and on their catalytic rates for H_2 production. Interestingly, the catalytic rates increase as the Ni(II/I) potentials become more positive. The overpotentials thus decrease with increasing activity, an unusual but beneficial trend. In addition, we report the effects of acid strength on H_2 production rates, and our observation that water enhances the catalytic rates for these complexes. Under the best conditions, turnover frequencies as high as 1850 s^{-1} have been observed for H_2 production at room temperature.

RESULTS

Synthesis and Characterization of Ligands and Complexes. The new and previously reported ligands used in this study were prepared using a single-flask two-step reaction (eq 1). In the first step a slight excess of two equivalents of paraformaldehyde was treated with phenylphosphine to form bis(hydroxymethyl)phenylphosphine. This step was followed by the addition of a solution of two equivalents of a para-substituted aniline in hot ethanol. The desired ligands precipitated as white solids upon cooling, and subsequent workup produced the ligands in reasonable yields and good purity. These ligands were characterized by ^1H and $^{31}P\{^1H\}$ NMR spectroscopy, elemental analyses, and mass spectroscopy, all of which are consistent with the structures indicated. The data for the new ligands are given in the Experimental Section.

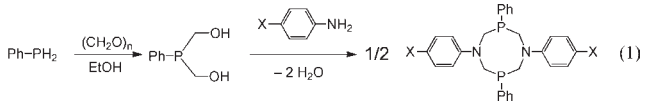

(1)

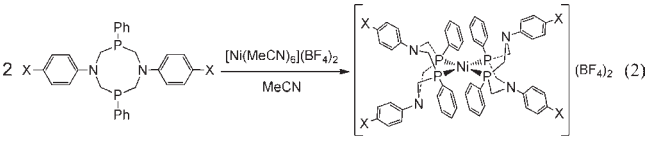

(2)

$[Ni(P^{Ph}{}_2N^{C6H4X}{}_2)_2](BF_4)_2$

The addition of two equivalents of a $P^{Ph}{}_2N^{C6H4X}{}_2$ ligand to an acetonitrile solution of $[Ni(Me_3CN)_6](BF_4)_2$ followed by workup provides a convenient synthesis of $[Ni(P^{Ph}{}_2N^{C6H4X}{}_2)_2](BF_4)_2$ (X = OMe, Me, $CH_2P(O)(OEt)_2$, H, Br, CF_3; eq 2). The $^{31}P\{^1H\}$ NMR spectra of these complexes all consist of one singlet resonance between 3 and 8 ppm, shifted by 50−55 ppm downfield upon coordination of the ligand to the metal. The simple ^1H NMR spectra indicate rapid interconversion between chair and boat conformations of the six-membered NiP_2C_2N rings. Elemental analyses and mass spectral data are also consistent with the proposed structures.

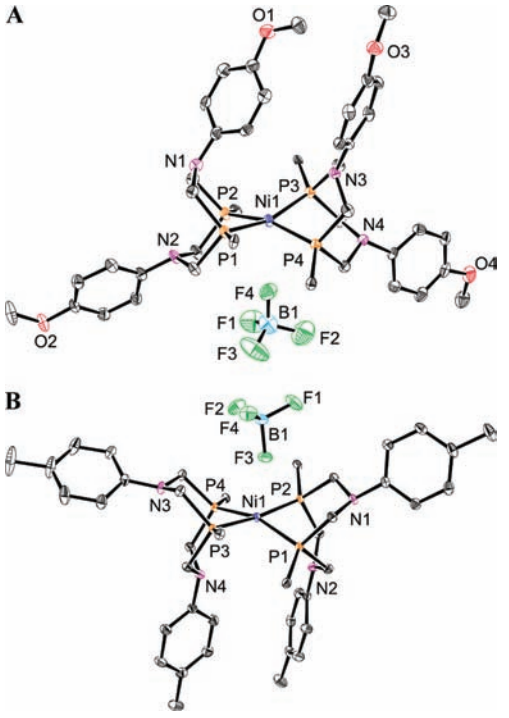

Figure 1. X-ray crystal structure diagrams of the dications of $[Ni(P^{Ph}{}_2N^{C6H4OMe}{}_2)_2](BF_4)_2$ (A) and $[Ni(P^{Ph}{}_2N^{C6H4Me}{}_2)_2](BF_4)_2$ (B), each showing the proximal BF_4^- counteranion. The distal BF_4^- counteranion and noncoordinating THF (for X = Me) and acetonitrile (for X = OMe) molecules are omitted for clarity. Only the *ipso* carbons of the phosphorus-bound phenyl rings are shown. Ellipsoids are plotted at the 50% confidence level.

Structural Studies. Dark-red crystals of $[Ni(P^{Ph}{}_2N^{C6H4OMe}{}_2)_2](BF_4)_2$ and $[Ni(P^{Ph}{}_2N^{C6H4Me}{}_2)_2](BF_4)_2$ were grown from a 3:1 THF:acetonitrile solution and a 20:1 THF:acetonitrile solution, respectively, by slow evaporation of the solvent under N_2 over several days. For $[Ni(P^{Ph}{}_2N^{C6H4OMe}{}_2)_2](BF_4)_2$ the crystals consist of discrete cations, tetrafluoroborate anions, and an unbound acetonitrile molecule. For $[Ni(P^{Ph}{}_2N^{C6H4Me}{}_2)_2](BF_4)_2$ the crystals consist of discrete cations, tetrafluoroborate anions, and two THF molecules. Drawings of the cations are shown in Figure 1, and a list of selected bond lengths and angles are given in Tables 1 and 2 for $Ni(P^{Ph}{}_2N^{C6H4OMe}{}_2)_2](BF_4)_2$ and $[Ni(P^{Ph}{}_2N^{C6H4Me}{}_2)_2](BF_4)_2$, respectively. The Ni−P bond lengths of 2.19−2.22 Å are typical for Ni(II) complexes with bidentate phosphine ligands, and the small P−Ni−P angles of 82−84° for the diphosphine ligands are also in the normal range observed for these bicyclic ligands.[10,11,14,15] The overall structures are best described as square planes with tetrahedral distortions resulting from a twisting of the diphosphine ligands to mitigate steric interactions between the phenyl groups on phosphorus. The dihedral angles between the P(1)−Ni(1)−P(2) plane defined by one diphosphine ligand and nickel and the P(3)−Ni(1)−P(4) plane defined by the other ligand and nickel are 24.16° for X = Me and 29.07° for X = OMe (Figure 1). This may be compared to a dihedral angle of 34.88° for $[Ni(P^{Cy}{}_2N^{Bz}{}_2)_2](BF_4)_2$[10] (Cy = cyclohexyl, Bz = benzyl), for which the steric interactions between adjacent P substituents are expected to be larger, and a dihedral angle of 2.4° for $[Ni(dmpe)_2](PF_6)_2$ (dmpe =1,2-bis(dimethylphosphino)ethane),[18] for which these steric interactions are smaller. In both structures, one BF_4^- ion is closer to Ni than the other, with one F atom oriented toward the Ni center. However, the Ni···F distances

dx.doi.org/10.1021/ja109755f |*J. Am. Chem. Soc.* 2011, 133, 5861–5872

Table 1. Selected Bond Distances and Angles for $[Ni(P^{Ph}_2N^{C6H4OMe}_2)_2](BF_4)_2$

bond distances (Å)		bond angles (°)	
Ni(1)−P(1)	2.1920(12)	P(1)−Ni(1)−P(3)	160.11(5)
Ni(1)−P(2)	2.2034(13)	P(1)−Ni(1)−P(2)	83.81(4)
Ni(1)−P(3)	2.1965(12)	P(3)−Ni(1)−P(2)	98.95(4)
Ni(1)−P(4)	2.2163(13)	P(1)−Ni(1)−P(4)	100.12(5)
Ni(1)···N(1)	3.405	P(3)−Ni(1)−P(4)	83.61(4)
Ni(1)···N(2)	3.770	P(2)−Ni(1)−P(4)	161.33(5)
Ni(1)···N(3)	3.310		
Ni(1)···N(4)	3.771		

Table 2. Selected Bond Distances and Angles for $[Ni(P^{Ph}_2N^{C6H4Me}_2)_2](BF_4)_2$

bond distances (Å)		bond angles (°)	
Ni(1)−P(1)	2.1962(4)	P(1)−Ni(1)−P(3)	97.731(16)
Ni(1)−P(2)	2.1886(4)	P(2)−Ni(1)−P(3)	170.515(18)
Ni(1)−P(3)	2.2071(4)	P(2)−Ni(1)−P(4)	99.894(16)
Ni(1)−P(4)	2.1947(4)	P(4)−Ni(1)−P(3)	83.670(16)
Ni(1)···N(1)	3.783	P(2)−Ni(1)−P(1)	82.107(15)
Ni(1)···N(2)	3.330	P(4)−Ni(1)−P(1)	159.093(18)
Ni(1)···N(3)	3.795		
Ni(1)···N(4)	3.154		

(2.98 Å for X = OMe and 2.62−2.67 Å for X = Me, having a disordered BF_4^-) of the closest BF_4^- anion are more than 0.4 Å longer than the sum of the covalent radii, 1.88 Å (Figure 1),[19] suggesting that cation−anion interactions in the solid state likely arise from electrostatic/packing effects rather than coordinative interactions. In both structures, the closer BF_4^- anion is accommodated by the conformations of the adjacent six-membered Ni-chelate rings, with these rings assuming chair conformations and the opposing rings adopting boat conformations.

Cyclic Voltammetry Studies of $[Ni(P^{Ph}_2N^{C6H4X}_2)_2](BF_4)_2$ Complexes. Each of the $[Ni(P^{Ph}_2N^{C6H4X}_2)_2](BF_4)_2$ complexes used in this study shows two distinct and reversible reduction waves assigned to the Ni(II/I) and Ni(I/0) couples. All redox potentials, reported vs the Cp_2Fe^+/Cp_2Fe couple, and ΔE_p values are presented in Table 3. Plots of the peak currents (i_p) versus the square root of the scan rate are linear for both waves, indicating that these redox reactions are diffusion controlled.[20] As the electron-donating ability of the para substituent increases, as measured by the pK_a values of the corresponding anilinium salt,[21−23] the potentials of both the Ni(II/I) and Ni(I/0) couples become more negative (Figure 2). Values of $E_{1/2}$ for the Ni(II/I) couples range from −0.74 V for X = CF_3 to −0.88 V for X = OMe. Values of $E_{1/2}$ for the Ni(I/0) couples range from −0.89 V for X = CF_3 to −1.07 V for X = OMe. The linear relationships in Figure 2 indicate that there is effective electronic communication between Ni and the para substituents on the phenyl rings, which are eight bonds away.

Catalytic Hydrogen Production. The complexes $[Ni(P^{Ph}_2N^{C6H4X}_2)_2](BF_4)_2$ (X = OMe, Me, H, $CH_2P(O)(OEt)_2$, Br, CF_3) are all active as electrocatalysts for H_2 production using Brønsted acid substrates. Their activities were measured by successive cyclic voltammograms of reaction mixtures for which the acid concentrations were systematically increased until the

Table 3. Electrochemical Data for $[Ni(P^{Ph}_2N^{C6H4X}_2)_2](BF_4)_2$ Complexes in Acetonitrile (0.2 M $Et_4N^+BF_4^-$)[a]

	Ni(II/I)		Ni(I/0)	
X	$E_{1/2}$ (V)	ΔE_p (mV)	$E_{1/2}$ (V)	ΔE_p (mV)
OMe	−0.88	67	−1.07	74
Me	−0.84	74	−1.05	73
$CH_2P(O)(OEt)_2$	−0.84	73	−1.02	72
H	−0.83	71	−1.02	76
Br	−0.79	63	−0.97	74
CF_3	−0.74	78	−0.89	64

[a] Referenced to the Cp_2Fe^+/Cp_2Fe couple.

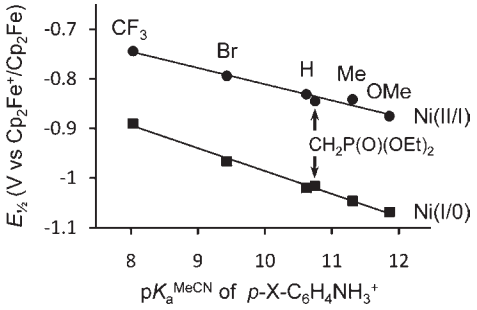

Figure 2. $E_{1/2}$ for Ni(II/I) and Ni(I/0) couples of $[Ni(P^{Ph}_2N^{C6H4X}_2)_2](BF_4)_2$ complexes as a function of pK_a^{MeCN} for the protonated form of the para-substituted aniline *p*-X-$C_6H_4NH_2$ from which the ligand is derived.

ratio i_{cat}/i_p of the catalytic current (i_{cat}) to the peak current of the Ni(II/I) reduction wave in the absence of acid (i_p) remained constant (the acid-independent region). Figure 3A shows a typical series of voltammograms obtained with increasing acid concentrations, and Figure 3B shows a corresponding plot of the catalytic current enhancement, i_{cat}/i_p, vs [acid]. From Figure 3B it can be seen that i_{cat}/i_p shows a strong dependence on acid concentration at low acid concentrations, but this ratio becomes independent of the acid concentration above approximately 0.2 M. The potential at which i_{cat} was measured was located by finding the potential negative of the potential of the Ni(II/I) couple for which the second derivative of the $i-E$ trace was approximately zero. These potentials were sufficiently negative to ensure quantitative reduction of Ni(II) species, 100−150 mV negative of $E_{1/2}$. At these potentials reduction of the acid by the electrode surface, onset of which is observed at ∼−1.9 V, was not a factor. The experimentally observed half-peak potentials for catalytic waves (E^{cat}) were within 50 mV of $E_{1/2}$ values for the corresponding Ni(II/I) couples. These results indicate that catalysis proceeds with reduction of the Ni(II) complex followed by protonation of the Ni(I) complex, consistent with the catalytic cycle proposed previously for catalysts of this class.[6,23]

Turnover frequencies were determined using eq 3 from i_{cat}/i_p values in the acid-independent region, as shown in Figure 3B.[23,24]

$$\frac{i_{cat}}{i_p} = \frac{n}{0.4463}\sqrt{\frac{RTk_{obs}}{Fv}} \qquad (3)$$

In eq 3 i_{cat} is the catalytic current measured in the presence of acid, i_p is the peak current for the Ni(II/I) redox couple measured in the absence of acid, n is the number of electrons involved in the

dx.doi.org/10.1021/ja109755f |J. Am. Chem. Soc. 2011, 133, 5861–5872

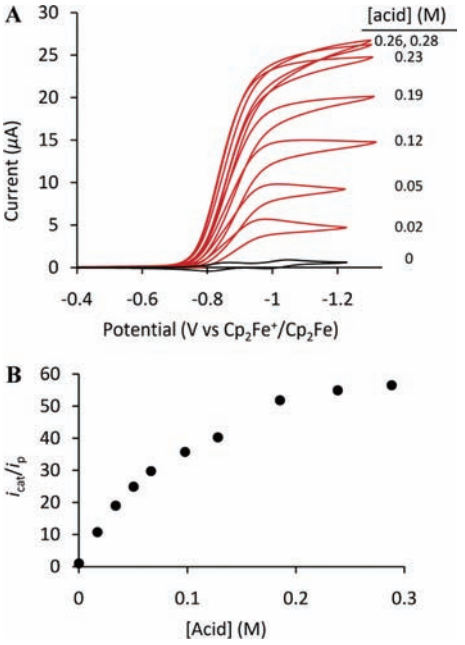

Figure 3. (A) Cyclic voltammograms of $[Ni(P^{Ph}{}_2N^{C6H4CH2P(O)(OEt)2}{}_2)_2](BF_4)_2$ (0.7 mM) in the absence of acid (black trace) and with varying concentrations of acid (acid = 1:1 DMF:$[(DMF)H]^+OTf^-$; red traces) in acetonitrile (0.2 M $Et_4N^+BF_4^-$). Scan rate ν = 50 mV/s. (B) Corresponding plot of i_{cat}/i_p vs acid concentration.

catalytic production of H_2, R is the gas constant, T is the temperature in K, F is the Faraday constant, ν is the scan rate in V/s, and k_{obs} is the observed rate constant. In the acid-independent region, the overall rate is first order in catalyst but independent of acid, and k is a first-order rate constant with units of s^{-1}, equivalent to the turnover frequency of the catalyst. The rate law under these conditions indicates that an intramolecular process is rate determining. Because NMR spectroscopy studies have shown that intramolecular proton exchange is fast (10^4–10^5 s^{-1} at 22 °C) for hydrogen oxidation catalysts of this class,[7,9] we have interpreted this slower unimolecular process to be associated with the elimination of H_2 from the nickel catalyst. The turnover frequencies determined for the entire series of catalysts studied here are summarized in Table 4. This table also includes data that shows how turnover frequencies are affected by different acids and by addition of water; these experiments are described in the following sections.

The overpotentials of these catalysts, calculated using the method of Evans et al.,[25] ranged from 220 to 370 mV depending on the catalyst and acid used (see values in parentheses in Table 4). Production of H_2 was established by quantitative gas chromatographic analysis of headspace gas obtained from a bulk electrolysis experiment using $[Ni(P^{Ph}{}_2N^{C6H4OMe}{}_2)_2](BF_4)_2$ (0.7 mM) with the working electrode held at −0.9 V in the presence of $[(DMF)H]^+OTf^-$ (0.23 M); the current efficiency was determined to be 94 ± 5%.

Effect of Acid on Catalytic Rates. In previous studies of $[Ni(P^{Ph}{}_2N^{Ph}{}_2)_2](BF_4)_2$ and $[Ni(P^{Ph}{}_2N^{Bz}{}_2)_2](BF_4)_2$ as catalysts for H_2 production, we used several different acids.[10,12,17] In our initial studies of $[Ni(P^{Ph}{}_2N^{Ph}{}_2)_2](BF_4)_2$, triflic acid was used because it is a strong acid with a poorly coordinating counterion that provided a good initial assessment of the activity of these complexes. However at high acid concentrations the strength of this acid resulted in catalyst decomposition. A solution of equimolar protonated dimethylformamide/dimethylformamide (1:1 DMF:$[(DMF)H]^+OTf^-$; pK_a^{MeCN} = 6.1)[26,27] was chosen as a weaker acid whose pK_a would more closely match the pK_a estimated for the protonated catalytic intermediate $[Ni(P^{Ph}{}_2N^{Ph}{}_2\boldsymbol{H})_2]^{2+}$, as described in more detail in the Discussion. Similarly, 4-bromoanilinium tetrafluoroborate was used to study the catalytic activity of $[Ni(P^{Ph}{}_2N^{Bz}{}_2)_2](BF_4)_2$, because its pK_a^{MeCN} (9.4) more closely matched the estimated pK_a^{MeCN} of $[Ni(P^{Ph}{}_2N^{Bz}{}_2\boldsymbol{H})_2]^{2+}$ (11.8) under catalytic conditions.[17] These studies clearly revealed the promising capabilities of these catalysts, but they did not provide systematic data for an evaluation of the dependence of the catalytic rates on N substituents or on the nature of the acid.

To explore how the nature of the acid influenced the catalytic rates for H_2 production, we carried out kinetic measurements for H_2 production for all of the complexes described in this paper using the following acids: $[(DMF)H]^+OTf^-$ (pK_a^{MeCN} = 6.1),[26] a 1:1 mol mixture of DMF and $[(DMF)H]^+OTf^-$ (1:1 DMF:-$[(DMF)H]^+OTf^-$), 4-cyanoanilinium tetrafluoroborate (pK_a^{MeCN} = 7.0),[28] and 2,6-dichloroanilinium triflate (pK_a^{MeCN} = 5.0).[21] The data presented in Table 4 show that the highest catalytic rates were observed for all complexes using $[(DMF)H]^+OTf^-$ as the acid. Catalytic activities were lower by 40–90% when 1:1 DMF:$[(DMF)H]^+OTf^-$ was used as the acid, and rates were further decreased by about an order of magnitude with either of the more sterically demanding anilinium acids. The pK_a values of the two anilinium acids bracket the pK_a value of $[(DMF)H]^+OTf^-$, the acid for which the highest catalytic rate is observed. As a result, it is clear that the catalytic rates do *not* parallel the pK_a values of the respective acids.

Effect of Substituents X on Catalytic Rates. As discussed in the Introduction, the previously studied $[Ni(P^{Ph}{}_2N^{Ph}{}_2)_2](BF_4)_2$ and $[Ni(P^{Ph}{}_2N^{Bz}{}_2)_2](BF_4)_2$ complexes exhibit significantly different rates for H_2 production, and this has been attributed to the different basicities of the two pendant amines. To explore the role of the basicity of the pendant amines in more detail, we have measured the catalytic rates of H_2 production for the acids described in the preceding paragraph for the $[Ni(P^{Ph}{}_2N^{C6H4X}{}_2)_2](BF_4)_2$ series of complexes. By varying the para substituent (X) of the pendant aniline base, it should be possible to probe the effect of changing the basicity at the N atom without significantly altering the steric properties of the catalyst. When $[(DMF)H]^+OTf^-$ was used as the acid, the $[Ni(P^{Ph}{}_2N^{C6H4X}{}_2)_2](BF_4)_2$ complexes showed activities increasing from 310 to 740 s^{-1} as the electron-withdrawing ability of X increased from OMe to Br, as shown in the first column of Table 4. A lower rate was observed for the CF_3 complex. Plots of the turnover frequency vs the pK_a values of the corresponding p-$XC_6H_4NH_3^+$ acids and of the turnover frequency vs the potentials of the Ni(II/I) couples are shown in Figure 4. The plots indicate a general increase in the rates as the pK_a values of the protonated aniline bases decrease and as the redox potentials of the catalysts become more positive. These trends are elaborated in the Discussion.

Effect of Water on Catalytic Rates. The addition of water (0.02 – 0.5 M) to reaction mixtures containing 0.20–0.45 M $[(DMF)H]^+OTf^-$ increased the catalytic rates by 30–60%. Figure 5 shows a representative example. The addition of larger concentrations of water (up to 2.4 M) to solutions containing the anilinium acids resulted in more significant rate increases (200–1400%, see Tables 4 and S1 and S2, Supporting

Table 4. Turnover Frequencies (TOF, s^{-1}) and Overpotentials (OP, mV, in Parentheses) for Electrocatalytic Hydrogen Production by $[Ni(P^{Ph}_2N^{C6H4X}_2)_2](BF_4)_2$ Complexes using Various Acids[a]

	$[(DMF)H]^+$ OTf^- pK_a^{MeCN} = 6.1		1:1 DMF:$[(DMF)H]^+$ OTf^- pK_a^{MeCN} = 6.1		2,6-$Cl_2C_6H_3NH_3^+$ OTf^- pK_a^{MeCN} = 5.0		4-$NCC_6H_4NH_3^+$ BF_4^- pK_a^{MeCN} = 7.0	
X	TOF	OP	TOF	OP	TOF	OP	TOF	OP
OMe	310	(310)	150	(330)	16	(330)	25	(270)
	480	*(330)*	*280*	*(350)*	*51*	*(360)*	*90*	*(330)*
Me	590	(340)	290	(310)	21	(320)	26	(290)
	770	*(360)*	*310*	*(320)*	*61*	*(370)*	*94*	*(350)*
$CH_2P(O)(OEt)_2$	500	(320)	290	(340)	31	(320)	16	(290)
	1850	*(370)*	*470*	*(350)*	*420*	*(350)*	*210*	*(290)*
H	590	(300)	270	(360)	31	(330)	28	(270)
	720	*(320)*	*480*	*(380)*	*160*	*(370)*	*72*	*(330)*
Br	740	(280)	120	(320)	36	(300)	14	(250)
	1040	*(290)*	*100*	*(330)*	*480*	*(360)*	*31*	*(270)*
CF_3	95	(300)	12	(290)	15	(330)	<1	(230)
	120	*(300)*	*12*	*(290)*	*15*	*(350)*	*3*	*(250)*

[a] Average of multiple runs. Values obtained after water was added are given in italics. Water concentrations giving maximum turnover frequencies ranged from 0.02 to 2.4 M. More complete information is available in the Supporting Information.

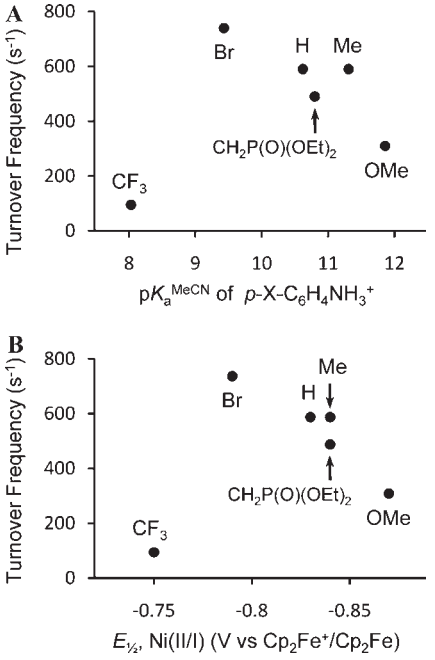

Figure 4. Turnover frequency (s^{-1}; obtained with $[(DMF)H]^+OTf^-$ as acid and with no added water) for electrocatalytic hydrogen production by $[Ni(P^{Ph}_2N^{C6H4X}_2)_2](BF_4)_2$ complexes: (A) as a function of pK_a^{MeCN} for the protonated form of the para-substituted aniline p-X-$C_6H_4NH_2$ from which the $P^{Ph}_2N^{C6H4X}_2$ ligand is derived, and (B) as a function of the potential of the Ni(II/I) couple.

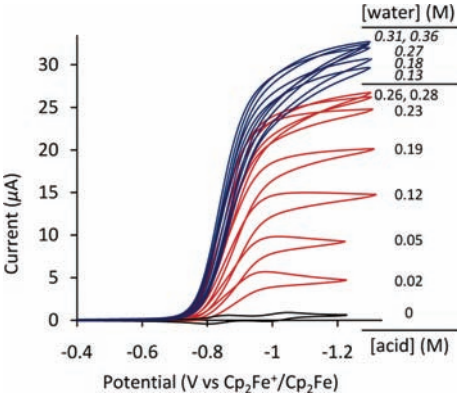

Figure 5. Cyclic voltammograms of $[Ni(P^{Ph}_2N^{C6H4CH2P(O)(OEt)2}_2)_2](BF_4)_2$ (0.7 mM) in the absence of acid (black trace), with varying [acid] (acid =1:1 DMF:$[(DMF)H]^+OTf^-$; red traces) and with varying [water] (blue traces, [acid] = 0.26 M), in acetonitrile (0.2 M $Et_4N^+BF_4^-$). Scan rate v = 50 mV/s. The acid concentration chosen for water addition was sufficient for acid independence in the absence of water.

Information). After the maximum current enhancement was reached in each case, the addition of further aliquots of water resulted in a decrease in catalytic activity. The largest proportional gain was realized for the phosphonate complex, X = $CH_2P(O)(OEt)_2$ and either 2,6-dichloroanilinium or 4-cyanoanilinium as the acid, and the largest turnover frequency, 1850 s^{-1}, was observed for the phosphonate complex using $[(DMF)H]^+OTf^-$ as the acid (350 mM) with added water (550 mM). Our initial reported turnover frequency of 350 s^{-1} for $[Ni(P^{Ph}_2N^{Ph}_2)_2](BF_4)_2$ titrated with 1:1 DMF:$[(DMF)H]^+OTf^-$ is bracketed by the values reported here for catalysis in the absence of water (270 s^{-1}) and in its presence (480 s^{-1}), suggesting the presence of trace quantities of adventitious water in prior experiments.[12]

The catalytic current was monitored as a function of water concentration to obtain kinetic data on the rate increases observed upon addition of water. Figure 6 shows plots of the observed catalytic rate as a function of water concentration along with fits to the experimental data according to a first-order and a second-order dependence on water concentration. In these kinetic studies, the concentration range over which water produces a measurable effect is small (0.05−0.2 M), and the resulting correlation coefficients for a linear fit (R^2 = 0.9916) and a square fit (R^2 = 0.9900) are similar, so a reaction order in [water] for the catalytic reaction has not been assigned.

dx.doi.org/10.1021/ja109755f |J. Am. Chem. Soc. 2011, 133, 5861–5872

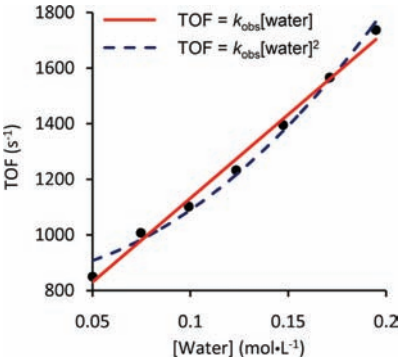

Figure 6. Turnover frequency (s^{-1}) as a function of water concentration, with $[Ni(P^{Ph}_2N^{C6H4CH2P(O)(OEt)2}_2)_2](BF_4)_2$ (0.7 mM) as catalyst and $[(DMF)H]^+OTf^-$ as acid in acetonitrile (0.2 M $Et_4N^+BF_4^-$): Experimental data (black points); least-squares line fits showing first-order (solid red line) and second-order (dashed blue line) dependence of turnover frequency on water concentration.

In some cases where water has been found to act as a cocatalyst, replacement of water with an alcohol has also been found to promote the catalytic reaction of interest.[29] When ethanol (0.23 M) was added to an electrolyte solution containing $[Ni(P^{Ph}_2N^{C6H4CH2P(O)(OEt)2}_2)_2](BF_4)_2$ and $[(DMF)H]^+OTf^-$, no current enhancement was observed. However, with 2,6-dichloroanilinium triflate as the acid, a 6-fold increase in the catalytic rate was observed with added ethanol (1.4 M). Under the same conditions, addition of water increased the turnover frequency by a factor of 14.

Effect of Dimethylformamide (DMF). ^{31}P NMR spectra and cyclic voltammograms of complexes $[Ni(P^{Ph}_2N^{C6H4CF3}_2)_2]^{2+}$ and $[Ni(P^{Ph}_2N^{C6H4Br}_2)_2]^{2+}$ in acetonitrile solutions showed that these complexes undergo ligand displacement in the presence of DMF. Dissolving $[Ni(P^{Ph}_2N^{C6H4CF3}_2)_2]^{2+}$ in pure DMF solutions resulted in the precipitation of a pale-green crystalline material attributed to $[Ni(DMF)_6](BF_4)_2$. In acetonitrile solutions with lower concentrations of DMF, both $[Ni(P^{Ph}_2N^{C6H4CF3}_2)_2]^{2+}$ and the free ligand were observed by ^{31}P NMR. This equilibrium process may contribute to the low catalytic rate observed for this complex with 1:1 DMF:$[(DMF)H]^+OTf^-$. However, there was *no* evidence for ligand dissociation for either $[Ni(P^{Ph}_2N^{C6H4CF3}_2)_2]^{2+}$ or $[Ni(P^{Ph}_2N^{C6H4Br}_2)_2]^{2+}$ for solutions containing pure $[(DMF)H]^+OTf^-$ or anilinium acids. This implies that unprotonated dimethylformamide is required for catalyst decomposition. For $[Ni(P^{Ph}_2N^{C6H4X}_2)_2]^{2+}$ complexes with substituents more electron donating than Br, no ligand dissociation was observed under catalytic conditions, even when 1:1 DMF:$[(DMF)H]^+OTf^-$ was used as the acid.

DISCUSSION

The three most significant findings from this study are: (1) For this series of catalysts, catalytic rates for H_2 production *increase* as the Ni(II/I) potentials become more positive. This trend is atypical of electrocatalytic reductions. (2) The dependence of the catalytic rate on acid size and on water suggests that catalyst activity depends on the site of protonation. (3) The outer coordination sphere, in addition to the first and second coordination spheres, also plays an important role in determining catalytic activity.

Previous mechanistic studies indicated that at high acid concentrations, the rate-determining step for H_2 production using $[Ni(P^{Ph}_2N^{Ph}_2)_2]^{2+}$ is independent of acid concentration and involves one or more steps in the elimination of H_2 from the diprotonated Ni(0) complex, $[Ni(P^{Ph}_2N^{C6H4X}_2\boldsymbol{H})_2]^{2+}$ (**3**) as shown in eq 4 (phosphorus and nitrogen substituents are omitted for clarity):[12,23]

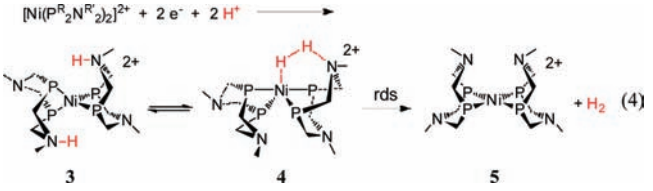

(4)

Theoretical studies of the reverse reaction, H_2 oxidation, by this class of catalysts suggested structure 4 as the transition state.[14,30] This structure suggests that hydrogen elimination should be favored by decreasing the basicity of the pendant amines (making the N−H more acidic) and increasing the hydride donor ability of the Ni(II) hydride.

Dependence of the Catalytic Rates for H_2 Production on X. In the current study we sought to explore the effect of changing the basicity of the pendant amines in $[Ni(P^{Ph}_2N^{Ph}_2)_2]^{2+}$ by changing para substituents on the aniline ring, while maintaining the hydride donor ability as constant as possible by using only the phenyl substituent on phosphorus. To this end, a series of $[Ni(P^{Ph}_2N^{C6H4X}_2)_2]^{2+}$ complexes with a wide range of electron-donor abilities for X have been synthesized and characterized. It can be seen from Figure 4B that the catalytic rates increase as the potentials of the catalysts become more positive. This is both unusual and beneficial. Positive shifts in catalyst potentials resulting from inductive effects typically lead to decreases in catalytic rates for reductive processes such as H_2 production,[31] CO_2 reduction,[32] or O_2 reduction.[33] The origin of the different behavior observed for the $[Ni(P^{Ph}_2N^{C6H4X}_2)_2]^{2+}$ catalysts described here is their bifunctional nature, in which both hydride and proton donors are incorporated in the same molecule. More positive potentials for the Ni(II/I) couples resulting from inductive effects will lead to a decrease in the hydride donor ability of transition state **4**, but this is offset by an even larger increase in the acidity of the protonated pendant amine. It is the *total* intramolecular driving force for H_2 elimination that affects the catalytic rate, and this does not necessarily parallel the reduction potential of the catalyst.

In acetonitrile, the difference in pK_a values between free anilinium ions (p-$XC_6H_4NH_3^+$) with the most electron-donating group, OMe (11.8),[21] and the most electron-withdrawing group, CF_3 (8.0),[21] is 3.8 pK_a units. A similar difference in pK_a values would be expected for the protonated pendant bases of the corresponding $[Ni(P^{Ph}_2N^{C6H4X}_2\boldsymbol{H})_2](BF_4)_2$ complexes, and this should provide an added driving force for H_2 elimination of 5.2 kcal/mol as X is varied from OMe to CF_3. Figure 4A shows a plot of the turnover frequency for H_2 production versus the pK_a of the corresponding anilinium acid, and it can be seen that the catalytic rates generally increase with the expected increase in the acidity of the protonated pendant amine.

This increase in acidity is partially offset by a decrease in the hydride donor ability. Because the potentials of the Ni(II/I) couples for the X = OMe and CF_3 derivatives differ by 0.14 V, the hydride donor ability of $[HNi(P^{Ph}_2N^{C6H4CF3}_2)_2](BF_4)$ should decrease by 2.7 kcal/mol relative to X = OMe, based on a

dx.doi.org/10.1021/ja109755f |*J. Am. Chem. Soc.* 2011, 133, 5861–5872

previously published linear free energy relationship between the Ni(II/I) potentials and the hydride donor abilities ($\Delta G^{\circ}_{H^-}$ = 19.2 $E_{1/2}$(II/I) + 77.3 kcal/mol).[17,34] As a result, the decrease in hydride donor ability attenuates the increase in driving force for H_2 elimination expected from differences in the acidities of the protonated pendant amines alone. However H_2 elimination is still expected to become more favorable by 2.5 kcal/mol (5.2−2.7 kcal/mol) as X is varied from OMe to CF_3. The catalytic rates should increase, and the potentials should shift more positive, reducing the overpotential. With the exception of the CF_3 complex (discussed further in the next section, Dependence of Catalytic Rates on Acid Strength), the results shown in Figure 4 and Table 4 agree with the expected trend. It is the acidity of the protonated pendant amine that dominates the driving force for H_2 elimination and determines the trend in catalytic rates for this series of complexes. This leads to the unusual increase in the catalytic rates for these complexes as the overpotentials decrease.

Dependence of Catalytic Rates on Acid Strength. The effect of acid strength on maximum turnover frequency has been tested by comparing anilinium salts of different acidities as substrates with the expectation that in the acid-independent region, the turnover frequency for a given catalyst will be independent of the pK_a of the acid. This is the case for X = OMe, Me, H, $CH_2P(O)(OEt)_2$, and Br. Within a factor of 2, the turnover frequencies are the same regardless of whether 2,6-dichloroanilinium triflate (2,6-Cl_2AnH$^+$OTf$^-$; pK_a^{MeCN} = 5.1)[21] or 4-cyanoanilinium tetrafluoroborate (pK_a^{MeCN} = 7.0)[28] is the substrate. However, for the catalyst with X = CF_3, the rate is similar to that observed for X = Br when the stronger acid 2,6-dichloroanilinium is used but is considerably slower with 4-cyanoanilinium as the acid. The less acidic 4-cyanoanilinium substrate does not effectively protonate the pendant bases of the intermediate complexes $[Ni(P^{Ph}_2N^{C6H4CF3}_2)_2]^+$ or $[HNi(P^{Ph}_2N^{C6H4CF3}_2)_2]^+$ under the conditions studied.

A more quantitative estimate of the basicity of the pendant amines in these complexes is instructive. The pK_a values of the protonated anilinium centers in the series of complexes studied here can be estimated by assuming a constant difference between these values in the nickel complexes (some of which have been experimentally determined) and the corresponding pK_a values for the free anilinium salts, p-$XC_6H_4NH_3^+$. In previous studies the pK_a^{MeCN} value of the $[Ni(P^{Ph}_2N^{C6H4X}_2\boldsymbol{H})_2]^{2+}$ intermediate (see structure **3** of eq 4) was estimated to be 5.6[17] while the pK_a^{MeCN} of anilinium ion is 10.6.[21] Using this difference of 5.0 units and the reported pK_a^{MeCN} values for a series of anilinium salts, we obtain the following pK_a^{MeCN} estimates for the $[Ni(P^{Ph}_2N^{C6H4X}_2\boldsymbol{H})_2]^{2+}$ complexes: 6.8 (OMe); 6.2 (Me); 5.7 ($CH_2P(O)(OEt)_2$); 5.6 (H); 4.4 (Br); and 3.0 (CF_3). Although these values are estimates, they indicate that formation of $[Ni(P^{Ph}_2N^{C6H4X}_2\boldsymbol{H})_2]^{2+}$ intermediates would require relatively strong acids. Under catalytic conditions, acid concentrations as high as 100−200 times that of the catalyst are frequently employed, suggesting that acids weaker than those indicated by the estimated pK_a values of the corresponding $[Ni(P^{Ph}_2N^{C6H4X}_2\boldsymbol{H})_2]^{2+}$ intermediates could be used. However, 4-cyanoanilinium, with a pK_a^{MeCN} value of 7.0, would likely be ineffective as a proton donor for catalysis by the CF_3 complex, i.e., independence of the rate on acid concentration is not likely to be achieved under experimentally relevant conditions. Even $[(DMF)H]^+OTf^-$, with a pK_a^{MeCN} of 6.1, would not be expected to fully protonate this catalyst, even at relatively high concentrations. The low basicity, together with the weak coordinating ability of the CF_3-containing ligand and its tendency to be displaced by DMF, account for the low turnover frequencies observed for the catalyst with X = CF_3 under a variety of conditions.

Dependence of Catalytic Rates on the Nature of the Acid, Water, and Ethanol. Acetonitrile solutions of $[(DMF)H]^+OTf^-$ (pK_a^{MeCN} = 6.1)[26] or 1:1 DMF:$[(DMF)H]^+OTf^-$ gave maximum turnover frequencies far exceeding those obtained with the anilinium acids, even though the pK_a value of $[(DMF)H]^+$ lies between those of 2,6-dichloroanilinium and cyanoanilinium. With 1:1 DMF:$[(DMF)H]^+OTf^-$, activities were up to 14 times greater than with the anilinium salts, and with $[(DMF)H]^+OTf^-$, activities were between 10 and 50 times greater. These results clearly indicate that the structure of the acid has a substantial impact on catalytic rates even at high acid concentrations where the catalytic rates are independent of acid. In this concentration range the rate-determining step is thought to be the elimination of H_2 from a diprotonated Ni(0) intermediate (eq 4). For systems that catalyze H_2 production, diprotonated Ni(0) intermediates are unstable with respect to H_2 elimination (e.g., by an estimated 9 kcal/mol for $[Ni(P^{Ph}_2N^{Ph}_2\boldsymbol{H})_2]^{2+}$), as a result they have not been detected spectroscopically. However, analogous intermediates have been characterized for related H_2 oxidation catalysts by experimental[12,14] and computational results.[14,30] Upon addition of H_2 to $[Ni(P^{Cy}_2N^{Bz}_2)_2]^{2+}$ (Cy = cyclohexyl, Bz = benzyl), three isomeric forms of the first observable intermediate, the diprotonated Ni(0) complex $[Ni(P^{Cy}_2N^{Bz}_2\boldsymbol{H})_2]^{2+}$, shown by structures **3**, **7**, and **8** (eq 5; Cy and Bz substituents not shown), have been characterized by multinuclear NMR studies. These isomers differ in the sites of protonation and in the conformations of the protonated six-membered chelate rings.

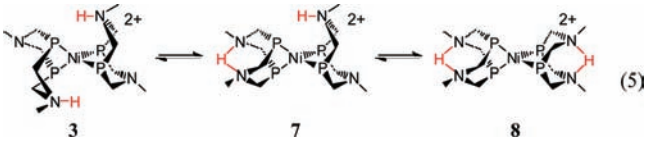

3 **7** **8** (5)

Similar isomers are likely to be formed upon protonation of Ni(0) intermediates in the H_2 production cycle, but only isomer **3** can continue to evolve as shown in eq 4 to form the proposed nickel hydride/protonated amine ($[HNi-NH]^{2+}$) transition state, **4**, followed by H_2 evolution. A similar pathway is not available for isomers **7** and **8**. The formation of the catalytically relevant isomer **3** requires two sequential protonations at N atoms in positions that are endo with respect to Ni. Protonation in the endo position is much less likely for sterically bulky acids, as can be appreciated from the structures shown in Figure 1 for $[Ni(P^{Ph}_2N^{C6H4Me}_2)_2]^{2+}$ and $[Ni(P^{Ph}_2N^{C6H4OMe}_2)_2]^{2+}$. As a result, it is expected that smaller acids would generate isomer **3** more rapidly or in greater amounts than bulkier acids, and this would lead to faster catalytic rates for $[(DMF)H]^+$ compared to the more sterically demanding acids 2,6-dicloroanilinium and 4-cyanoanilinium.

For all of the acids, the addition of water results in a further increase in the rates of H_2 formation catalyzed by the $[Ni(P^{Ph}_2N^{C6H4X}_2)_2]^{2+}$ complexes. This is consistent with the hydronium ion formed by protonation of water gaining greater access to the interior of the molecule, enhancing the formation of isomer **3**. It seems unlikely that added water increases the turnover frequency by changing either the dielectric of the solvent or the acidity of the solution, since addition of water produces very large catalytic enhancements even at low

dx.doi.org/10.1021/ja109755f |J. Am. Chem. Soc. 2011, 133, 5861–5872

concentrations where neither dielectric or acidity should change significantly. The highest water concentration at which optimal catalytic rates were obtained was 2.4 M (Table S3 of the Supporting Information), or ~4.3% v/v for the $[Ni(P^{Ph}{}_2N^{C6H4X}{}_2)_2]^{2+}$ complex having X = $CH_2P(O)(OEt)_2$ titrated with 4-cyanoanilinium tetrafluoroborate, with addition of water leading to a 1300% increase in turnover frequency. At 20 °C, a water−acetonitrile mixture having this composition is predicted to have ε = 38.56, a 5% increase compared to neat acetonitrile (ε = 36.67).[35] In addition, the different catalysts studied here respond differently to added water, suggesting that specific interactions between water and the catalyst are important, rather than medium effects such as changes to pH or dielectric constants.

It is also possible that the effect of water is related to its ability to serve as a proton relay and/or because of stabilizing effects of hydrogen bonding. Such mechanistic proposals for H−H bond formation or cleavage have been advanced for other systems containing intramolecular bases,[36] and such interactions may be important for the $[Ni(P^{Ph}{}_2N^{C6H4X}{}_2)_2]^{2+}$ complexes as well. In fact, the addition of ethanol enhances the catalytic rate as does water, albeit to a lesser degree. This effect is seen with 2,6-dichloroanilinium as substrate but not with $[(DMF)H]^+$, again supporting the idea that substrate size is critical in determining catalytic rate. The higher catalytic rates observed for smaller acids and the increased catalytic rates observed in the presence of water are consistent with formation of species such as **3** and **4.** The formation of these species requires that both protonation reactions of the doubly reduced $[Ni(P^{Ph}{}_2N^{C6H4X}{}_2)_2]^{2+}$ complexes occur in the endo positions with respect to Ni. If this interpretation is true, then only a small fraction of the catalyst may participate in the production of H_2. This suggests that further design refinements to increase endo protonation and prevent exo protonation could produce significantly more active catalysts than the best catalyst reported here, which has a turnover frequency of 1850 s^{-1} for H_2 production and is in the 700−9000 s^{-1} range reported for [NiFe] and [FeFe] hydrogenases.[2]

Dependence of Catalytic Rates on the Outer Coordination Sphere. The largest turnover frequencies were obtained with $[(DMF)H]^+OTf^-$ as substrate and with water added to the reaction mixtures. Under these conditions, $[Ni(P^{Ph}{}_2N^{C6H4CH2P(O)(OEt)2}{}_2)_2](BF_4)_2$ has a rate of 1850 s^{-1}, the highest reported thus far for this class of catalysts. On the basis of inductive effects, the phosphonate derivative, $[Ni(P^{Ph}{}_2N^{C6H4CH2P(O)(OEt)2}{}_2)_2](BF_4)_2$, would be expected to have a turnover frequency slightly lower than that of $[Ni(P^{Ph}{}_2N^{Ph}{}_2)_2](BF_4)_2$. This is true when protonated dimethylformamide is used as the acid (see Figure 4 and Table 4). However, in the presence of both acid and water, $[Ni(P^{Ph}{}_2N^{C6H4CH2P(O)(OEt)2}{}_2)_2](BF_4)_2$ is more than twice as fast as $[Ni(P^{Ph}{}_2N^{Ph}{}_2)_2](BF_4)_2$. This result indicates that groups such as phosphonate, located in the outer coordination sphere of these molecules, can exert a significant influence on the catalytic rate even though they are far from the catalytic site. This also suggests that further modification of the outer coordination sphere to control the delivery of protons to endo positions may be a fruitful avenue for further improvement of these catalysts.

SUMMARY AND CONCLUSIONS

Previous studies of nickel and cobalt catalysts containing diphosphine ligands with and without pendant amines have demonstrated the importance of the pendant amines in improving catalyst performance in terms of overpotentials and rates. In addition, positioned pendant amines improve catalytic rates significantly compared to catalysts with nonpositioned pendant amines. To study the effect of the acidity of the pendant amine on catalytic activity, a series of complexes of the formula $[Ni(P^{Ph}{}_2N^{C6H4X}{}_2)_2]^{2+}$, where the *para*-aniline substituent X = OMe, Me, H, $CH_2P(O)(OEt)_2$, Br, and CF_3, were synthesized and characterized. The turnover frequencies for this series of catalysts are increased by electron-withdrawing para substituents, which favor the release of H_2 in the catalytic cycle. Increasing the electron-withdrawing nature of the para substituents of the pendant base also results in more positive potentials for the Ni(II/I) couple at which catalysis occurs. Consequently, the favorable but unusual behavior is observed in which the turnover frequency increases as the overpotential decreases. This behavior is expected to be more common for bifunctional catalysts for H_2 production that have both hydride and proton donors incorporated in the same molecule.

In this work it is also demonstrated that the size of the acid as well as the presence of water has a significant influence on turnover frequencies. The dependence on size and water are attributed to the preference of smaller acids to protonate at the catalytically active endo positions of the catalyst. This suggests that controlling the delivery of protons to endo sites should further increase the rates of these catalysts; such studies are currently in progress.

Finally, in the presence of $[(DMF)H]^+OTf^-$ and water, $[Ni(P^{Ph}{}_2N^{C6H4CH2P(O)(OEt)2}{}_2)_2]^{2+}$ has a turnover frequency of 1850 s^{-1}, more than twice as fast as for the electronically comparable $[Ni(P^{Ph}{}_2N^{Ph}{}_2)_2]^{2+}$ catalyst and in the 700−9000 s^{-1} range reported for [NiFe] and [FeFe] hydrogenases.[2] These rates are the highest reported thus far for this class of catalysts, and they suggest that, in addition to the first and second coordination spheres, the outer coordination sphere can also be used to enhance catalyst performance.

EXPERIMENTAL SECTION

Materials and Methods. All manipulations were carried out using standard Schlenk or inert-atmosphere glovebox techniques using oven-dried glassware, unless otherwise indicated. THF (Alfa-Aesar, anhydrous, nonstabilized), acetonitrile (Alfa-Aesar, anhydrous, amine-free), and ether (Burdick & Jackson) were purified by sparging with N_2 and passage through neutral alumina, and ethanol (Pharmco-Aaper absolute anhydrous) was purified by sparging with N_2 and passage through calcium sulfate, using a solvent purification system (PureSolv, Innovative Technologies, Inc.). Dimethylformamide (Burdick & Jackson) was dried over activated 4 Å molecular sieves. Ethyl acetate (Aldrich) was used as received. Acetonitrile-d_3 (Cambridge Isotope Laboratories, 99.5% D) was vacuum-distilled from P_2O_5. Chloroform-*d* (Cambridge Isotope Laboratories, 99.5% D) was used as received. Tetraethylammonium tetrafluoroborate (Alfa-Aesar) was recrystallized from hot ethanol and dried under vacuum. Trifluoromethanesulfonic acid (Aldrich, 99%) was used as received and handled under nitrogen. Dimethylformamide-trifluoromethanesulfonic acid, $[(DMF)H]^+OTf^-$, was prepared by the method of Favier and Duñach.[37] Water was dispensed from a Millipore Milli-Q purifier and sparged with nitrogen. Ferrocene (Aldrich) was sublimed under vacuum before use. Phenylphosphine (Strem, 99%) paraformaldehyde (Aldrich, 95%), diethyl *para*-aminobenzylphosphonate (Acros, 98%), and *para*-trifluoromethylaniline (Aldrich, 99%) were used as received; *para*-anisidine (Aldrich 99%) was sublimed before use.

$[Ni(MeCN)_6](BF_4)_2 \cdot 1/2$ MeCN,[38] $P^{Ph}{}_2N^{C6H4Br}{}_2$, and $P^{Ph}{}_2N^{C6H4Me}{}_2$ were prepared using literature methods.[39]

Instrumentation. ^{1}H and ^{31}P NMR spectra were recorded on a Varian Inova spectrometer (500 MHz for ^{1}H) at 23 °C unless otherwise noted. Residual ^{1}H signals for each deuterated solvent were used as internal references, and all ^{1}H chemical shifts are referenced to tetramethylsilane. The ^{31}P NMR spectra were referenced to external phosphoric acid. Electrospray ionization (ESI) and chemical ionization (CI) mass spectra were collected at the Indiana University Mass Spectrometry Facility on a Waters/Micromass LCT Classic using anhydrous solvents and inert atmosphere techniques. Elemental analyses were carried out by Atlantic Microlab, Norcross, GA. All electrochemical experiments were carried out under an atmosphere of acetonitrile-saturated nitrogen in 0.2 M acetonitrile solutions of $Et_4N^+BF_4^-$ using ferrocene as an internal standard, and all potentials are referenced to the ferricenium/ferrocene couple at 0.0 V. Cyclic voltammograms were acquired using a CH Instruments 620D or 660C potentiostat equipped with a standard three-electrode cell. Prior to the acquisition of each cyclic voltammogram, the working electrode (1 mm PEEK-encased glassy carbon, Cypress Systems EE040) was polished using 0.1 μm γ-alumina (BAS CF-1050) suspended in water, and then rinsed with water, acetone, and finally with dry acetonitrile dispensed under a flow of nitrogen. A 3 mm glassy carbon rod (Alfa) was used as the counter-electrode, and a silver wire suspended in electrolyte solution and separated from the analyte solution by a Vycor frit (CH Instruments 112) was used as a pseudoreference electrode. Controlled potential electrolyses were performed using a CH Instruments 1100A power potentiostat. Gas analysis for H_2 was performed using a Agilent 6850 gas chromatograph fitted with a 10 ft long Supelco 1/8" Carbosieve 100/120 column, calibrated with two H_2/N_2 gas mixtures of known composition.

Syntheses. *$P^{Ph}{}_2N^{C6H4OMe}{}_2$.* A 250 mL Schlenk flask was charged with phenylphosphine (1.87 g, 17.0 mmol), paraformaldehyde (1.10 g, 36.6 mmol) and 25 mL of degassed absolute ethanol. The resulting suspension was immersed in a hot oil bath (65 °C) and stirred for 12 h resulting in a clear solution. A degassed solution of *para*-anisidine (2.09 g, 17.0 mmol) in 10 mL ethanol was added dropwise to the hot solution over a period of 30 min. The resulting white suspension was heated for 2 h at 60 °C. The reaction mixture was cooled to room temperature, the solvent volume reduced on a vacuum line to 20 mL, and the white solid product was collected by filtration and dried in vacuo (2.54 g, 4.94 mmol, 58%). ^{31}P{^{1}H} NMR ($CDCl_3$): δ −50.21. ^{1}H NMR ($CDCl_3$): δ 7.61 (m, 4H, Ar*H*); 7.49 (m, 6H, Ar*H*); 6.83 (m, 4H, Ar*H*); 6.67 (m, 4H, Ar*H*); 4.21 (m) and 3.99 (m, 8H total, PCH_2N); 3.71 (s, 6H, OCH_3). Analysis calculated for $C_{30}H_{32}N_2P_2O_2$: C, 70.02%; H, 6.26%; N, 5.44%. Found: C, 69.88%; H, 6.35%; N, 5.53%. CI-MS: Observed M^+ at 514.1912, predicted 514.1934.

$P^{Ph}{}_2N^{C6H4CH2P(O)(OEt)2}{}_2$. Phenylphosphine (2.22 g, 20.2 mmol) and paraformaldehyde (1.256 g, 45.95 mmol) were combined in 10 mL of ethanol and heated with stirring to 60−65 °C for 2 h at which point the mixture had become almost clear. The mixture was then warmed to 85 °C for 4 h and held at 70 °C for 12 h to ensure complete reaction before cannula transferring a 25 mL ethanol solution of diethyl *para*-aminobenzylphosphonate (4.907 g, 20.17 mmol) to the reaction mixture. The reaction mixture was held at 70 °C for 2 h before removing the solvent, and the residue was transferred to a glovebox for the remaining workup. The residue was stirred with 40 mL of THF forming a white solid and a yellow solution. The solid was collected on a frit, rinsed with ether, and dried in vacuo (5.773 g, 7.65 mmol, 75%). Addition of 60 mL of ether to the filtrate solution resulted in the formation of a light-yellow solid (0.549 g, 0.73 mmol, 7.2%). The combined solids were purified by crystallization from a mixture of acetonitrile and ether. ^{31}P{^{1}H} NMR (CD_3CN): δ −52.5 (CH_2PPhCH_2); 27.4 ($P(O)(OEt)_2$). ^{1}H NMR (CD_3CN): δ 7.67 (m, 4H, Ph); 7.48 (m, 6H, Ph); 7.06 (dd, J = 9.2 Hz, 4H, Ph); 6.70 (dd J = 2 Hz, 4H, Ph); 4.26 (m, 8H, PCH_2N); 3.93 (dq, J = 8, 7 Hz, 8H, OCH_2CH$_3$); 2.96 3.13 (d, J = 21 Hz, 4H, PhCH_2P); 1.18 (t, J = 7 Hz, 12H, OCH$_2$CH_3). CHN Anal. calcd for $C_{38}H_{50}N_2O_6P_4$: C, 60.47; H, 6.68; N, 3.71. Found: C, 60.48; H, 6.68; N, 3.76%.

$P^{Ph}{}_2N^{C6H4CF3}{}_2$. A 250 mL Schlenk flask was charged with phenylphosphine (1.79 g, 16.2 mmol), paraformaldehyde (0.990 g, 33.0 mmol), and 25 mL of ethanol. The resulting suspension was held at 65 °C and stirred for 12 h, forming a clear solution. A solution of *para*-trifluoromethylaniline (2.62 g, 16.3 mmol) in 10 mL ethanol was added dropwise to the hot solution over a period of 30 min. Completion of the addition resulted in a white suspension that was heated for 2 h at 45 °C. The mixture was cooled to room temperature, the solvent volume reduced on a vacuum line to 20 mL, and the white solid product was collected by filtration and dried in vacuo (3.74 g, 6.33 mmol, 78%). ^{31}P{^{1}H} NMR ($CDCl_3$,): δ −48.09. ^{1}H NMR ($CDCl_3$): δ 7.62 (m, 4H, Ar*H*); 7.55 (m, 6H, Ar*H*); 7.42 (d, J = 9 Hz, 4H, Ar*H*); 6.63 (d, J = 9 Hz, 4H, Ar*H*); 4.46 (m) and 4.04 (dd, J = 16 Hz, 8H total, PCH_2N). Anal. calcd for $C_{30}H_{26}N_2P_2F_6$: C, 61.02%; H, 4.44%; N, 4.74%. Found: C, 60.97%; H, 4.35%; N, 4.85%. CI-MS: Observed M^+ at 590.1488, predicted 590.1475.

$[Ni(P^{Ph}{}_2N^{C6H4CF3}{}_2)_2](BF_4)_2$. Two equivalents of $P^{Ph}{}_2N^{C6H4CF3}{}_2$ (1000 mg, 1.694 mmol) were added to a solution of $[Ni(MeCN)_6](BF_4)_2 \cdot 1/2$MeCN (422 mg, 0.845 mmol) in acetonitrile (15 mL). After stirring overnight, the resultant red solution was filtered through a plug of Celite. The solvent was removed from the filtrate under vacuum. The red powder was washed with ether and dried in vacuo (1.15 g, 0.814 mmol, 96%). ^{31}P{^{1}H} NMR (CD_3CN): δ 3.34 (s). ^{1}H NMR (CD_3CN): δ 7.61 (d, J = 8 Hz, 8H, Ar*H*); 7.44 (t, J = 7 Hz, 8H, Ar*H*); 7.25 (m, 16H, Ar*H*); 4.29 (d, J = 14 Hz, 8H, PCH_2N); 4.02 (broad, 8H, PCH_2N). Anal. calcd for $C_{60}H_{52}N_4P_4F_{20}NiB_2$: C, 50.99; H, 3.70; N, 3.96. Found: C, 50.73; H, 3.71; N, 4.15. ESI-MS: Observed $\{[Ni(P_2N_2)_2](BF_4)\}^+$ at m/z 1325.2352, predicted 1325.2334.

$[Ni(P^{Ph}{}_2N^{C6H4OMe}{}_2)_2](BF_4)_2$. This complex was prepared in a manner analogous to that described for $[Ni(P^{Ph}{}_2N^{C6H4CF3}{}_2)_2](BF_4)_2$ and was isolated as a red powder in 97% yield. ^{31}P{^{1}H} NMR (CD_3CN): δ 6.10 (s). ^{1}H NMR (CD_3CN): δ 7.31 (m, Ar*H,* 12H); 7.22 (d, J = 9 Hz, Ar*H,* 8H); 7.10 (t, J = 9 Hz, Ar*H,* 8H); 6.93 (d, J = 9 Hz, Ar*H,* 8H); 4.11 (d, J = 14 Hz, PCH_2N, 8H); 3.78 (broad, PCH_2N, 8H) 3.76 (s, OCH_3, 12H). ESI-MS: Observed $\{[(Ni(P_2N_2)_2](BF_4)\}^+$ at m/z 1173.3257, predicted 1173.3261.

$[Ni(P^{Ph}{}_2N^{C6H4Me}{}_2)_2](BF_4)_2$. This complex was prepared in a manner analogous to that described for $[Ni(P^{Ph}{}_2N^{C6H4CF3}{}_2)_2](BF_4)_2$ and was isolated as a red powder in 94% yield. ^{31}P{^{1}H} NMR (CD_3CN): δ 5.44 (s). ^{1}H NMR (CD_3CN): δ 7.35 (t, J = 7 Hz, 8H, Ar*H*); 7.29 (m, 8H, Ar*H*); 7.20 − 7.09 (m, 20H, Ar*H*); 4.18 (d, J = 14 Hz, 8H, PCH_2N); 3.83 (d, J = 14 Hz, 8H, PCH_2N) 2.31 (s, 12H, ArCH_3). ESI-MS: Observed $\{[(P_2N_2)_2Ni](BF_4)\}^+$ at m/z 1109.3486, predicted 1109.3474.

$[Ni(P^{Ph}{}_2N^{C6H4Br}{}_2)_2](BF_4)_2$. This complex was prepared in a manner analogous to that described for $[Ni(P^{Ph}{}_2N^{C6H4CF3}{}_2)_2](BF_4)_2$ and was isolated as a red powder in 98% yield. ^{31}P{^{1}H} NMR (CD_3CN): δ 4.9 (s). ^{1}H NMR (CD_3CN): δ 7.47 (d, J = 9 Hz, 8H, Ar*H*); 7.36 (t, J = 7 Hz, 4H, Ar*H*); 7.23 (m, 8H, Ar*H*); 7.11 (m, 16H, Ar*H*); 4.14 (d, J = 14 Hz, 8H, PCH_2N); 3.85 (m (broad), 8H, PCH_2N). ESI-MS: Observed $[Ni(P_2N_2)_2]^+$ at m/z 1281.9147, predicted 1281.9189.

$[Ni(P^{Ph}{}_2N^{C6H4CH2P(O)(OEt)2}{}_2)_2](BF_4)_2$. $P^{Ph}{}_2N^{C6H4CH2P(O)(OEt)2}{}_2$ (0.651 g, 0.862 mmol) and $[Ni(NCMe)_6](BF_4)_2 \cdot 1/2$ MeCN (0.218 g, 0.437 mmol) were combined in 10 mL of acetonitrile, and the resulting dark-red solution was stirred for 48 h before filtering through Celite and removing the solvent in vacuo. The oily residue was stirred with 20 mL of ether for 72 h to produce a fine pink suspended solid that was collected on a frit, washed with 20 mL of ether, and dried in vacuo (0.526 g, 0.302 mmol, 70%). The oily residue remaining after stirring in ether was dissolved in 5 drops of acetonitrile, and 10 mL of ether was added, precipitating an oil. The mixture was stirred for 72 h to get a fine pink

suspended solid that was collected on a frit, washed with 20 mL of ether, and dried in vacuo to obtain (0.104 g, 0.060 mmol, 14%) of additional product. $^{31}P\{^1H\}$ NMR (CD_3CN): δ 5.0 (CH_2PPhCH_2); 27.6 ($P(O)(OEt)_2$).^1H NMR (CD_3CN): δ 7.40 (t, J = 7 Hz, 4H, Ph); 7.33 − 7.25 (m, 16H, Ph); 7.15 (m, 16H, Ph); 4.19 (d, J = 14 Hz, 8H, PCH_2N); 3.97 (d of q, J = 8, 7 Hz, 16H, OCH_2CH_3); 3.91(m, 8H, PCH_2N); 3.13 (d, J = 21 Hz, 8H, $PhCH_2P$); 1.18 (t, J = 7 Hz, 24H, OCH_2CH_3). ESI-MS: Observed $\{[(P_2N_2)_2Ni](BF_4)\}^+$ at m/z 1653.4564, predicted 1653.4621.

Determination of pK_a^{MeCN} for Diethyl 4-Aminobenzylphosphonate. Anilinium tetrafluoroborate was isolated as an oil by reacting aniline (0.122 g, 0.502 mmol) with tetrafluoroboric acid etherate (0.1 mL, ~0.57 mmol). Then CD_3CN (1.0 mL) was added to a mixture of 4-aminobenzylphosphonate (0.006 g, 0.02 mmol) and anilinium tetrafluoroborate (0.004 g, 0.02 mmol). Rapid interconversion was observed between anilinium and aniline ($PhNH_3^+$ and $PhNH_2$) and between 4-(diethyl phosphonomethyl)phenylammonium and 4-aminobenzylphosphonate ($NH_3C_6H_4CH_2P(O)(OEt)_2^+$ and $NH_2C_6H_4CH_2P(O)(OEt)_2$) by ^1H NMR, and the relative abundances at equilibrium were determined by comparing the observed ortho and meta aryl chemical shifts with those of the pure free bases and their respective conjugate acids: $NH_2C_6H_4CH_2P(O)(OEt)_2$: δ 6.97, 6.57; $NH_3C_6H_4CH_2P(O)(OEt)_2^+$: δ 7.32, 7.21; $PhNH_2$: δ 7.08, 6.63; $PhNH_3^+$: δ 7.53, 7.39. The observed exchange-averaged chemical shifts for $NH_2C_6H_4CH_2P(O)(OEt)_2$/ $NH_3C_6H_4CH_2P(O)(OEt)_2^+$: δ 7.08, 6.76, correspond to a mole ratio of 0.69. Similarly the average chemical shifts observed for $PhNH_2/PhNH_3^+$: δ 7.19, 6.81, correspond to a mole ratio of 0.76. From this data, the equilibrium constant K_{eq} = $[PhNH_2][NH_3C_6H_4CH_2P(O)(OEt)_2^+]/[PhNH_3^+][NH_2C_6H_4CH_2P(O)OEt)_2]$ was calculated to be 1.4. The experiment was repeated twice more using 0.012 g (0.049 mmol) of $NH_2C_6H_4CH_2P(O)(OEt)_2$ and 0.006 g (0.003 mmol) $PhNH_3BF_4$ as well as 0.004 g (0.02 mmol) of $NH_2C_6H_4CH_2P(O)(OEt)_2$ and 0.002 g (0.01 mmol) of $PhNH_3BF_4$ to obtain a K_{eq} value of 1.4 in both cases. The pK_a^{MeCN} of $NH_3C_6H_4CH_2P(O)(OEt)_2^+$ is 10.8, the sum of the pK_a^{MeCN} of $PhNH_3^+$ (10.62)[21] and log K_{eq}.

Catalytic Hydrogen Production. *Determination of Rate and Overpotential.* All catalytic experiments were carried out at ambient temperature, 22 °C. Solutions of electrolyte (0.2 M $Et_4N^+BF_4^-$ or $^nBu_4N^+OTf^-$ in acetonitrile), analyte (~0.5 mM catalyst in electrolyte solution), and titrant (~1.7 M acid in acetonitrile) were prepared in the glovebox. Absence of moisture from a sample electrolyte solution (<1 ppm water) was established using a Karl Fischer coulometric titrator. Internal reference ferricenium/ferrocene was used to track analyte dilution due to titrant addition. A scan rate of 50 mV/s was used for all runs. Overpotentials were taken as the difference between E^{cat} and the thermodynamic potential $E°$ for the reduction of acid to free base plus one-half equivalent H_2 gas.[25] The potentials at which i_{cat} values were measured were located by finding the most positive potential for each catalytic wave beyond the $E_{1/2}$ of the Ni(II/I) couple for which the second derivative of the $i - E$ trace is approximately zero. These potentials were 100−150 mV negative of $E_{1/2}$. A representative experiment is given in the following section.

Using $[Ni(P^{Ph}{}_2N^{C6H4Me}{}_2](BF_4)_2$ as Catalyst and 1:1 DMF:[(DMF)H]$^+$OTf$^-$ as Acid. In a glovebox, $[Ni(P^{Ph}{}_2N^{C6H4Me}{}_2](BF_4)_2$ (1.1 mg, 0.92 μmol) was weighed into a 4 mL glass vial and dissolved in 2.0 mL acetonitrile (0.2 M tetraethylammonium tetrafluoroborate), then 5 μL of acetonitrile (0.054 M ferrocene) was added as internal reference. In a separate vial, $[(DMF)H]^+OTf^-$ (190 mg, 0.851 mmol) was weighed and dissolved in 0.50 mL acetonitrile. To this solution was added 60 μL (0.77 mmol) DMF. These vials were capped and removed from the box. The analyte solution vial was fitted with electrodes under a stream of acetonitrile-saturated nitrogen, and a baseline voltammogram was recorded. Titrant was transferred via microsyringe in 20−100 μL increments. Aliquot volumes were adjusted as required to obtain acid concentrations for which the catalytic current became constant within 15 additions, to minimize bias due to different catalyst stabilities. After each addition of titrant, the electrode was polished, and a voltammogram was recorded. Scans showing unusual line shape features, or catalytic half-peak potentials or current enhancements at significantly more negative values than prior runs, were repeated after thorough polishing of the electrode. Titration was continued until three successive additions resulted in no further increase in catalytic current enhancement. Once acid- independence was established, degassed water was admitted in 1 μL increments until the catalytic current stopped increasing. A similar procedure was used for other acids and catalysts studied.

Order with Respect to Water. To assess the reaction order of the catalyst enhancement with respect to added water, the peak current of solutions containing catalyst and acid were measured by cyclic voltammetry. Once the system had reached zero-order conditions in acid, a small volume (10 μL) of a 9:1 acetonitrile−water solution was added followed by manual stirring of the solution. The peak current of the system was then measured. This process was repeated until the peak current began to decrease.

Controlled Potential Coulometry. A three-necked flask having a total volume of 150 mL was used as the bulk electrolysis vessel and was assembled under a flow of nitrogen with each neck accepting an electrode fed through a pierced rubber septum. The working electrode consisted of a copper wire attached to a reticulated vitreous carbon cylinder; the reference and counter electrodes were a Ag wire and graphite rod, respectively, placed into 5 mm glass tubes terminating in Vycor fritted disks and filled with acetonitrile (0.1 M $Et_4N^+BF_4^-$) electrolyte solution. A solution of $[Ni(P^{Ph}{}_2N^{C6H4OMe}{}_2)_2](BF_4)_2$ (12 mg, 9.5 μmol), ferrocene, and $Et_4N^+BF_4^-$ (990 mg, 4.6 mmol) in 10 mL acetonitrile and a solution of $[(DMF)H]^+OTf^-$ (742 mg, 3.3 mmol) in 5 mL acetonitrile were prepared in the glovebox. The catalyst/ferrocene solution was then transferred to the reaction vessel via syringe, and a cyclic voltammogram was obtained. The acid solution was then added, and controlled potential coulometry was performed at −0.90 V versus the ferricenium/ferrocene internal reference. After 29.3 C of charge was passed, a 200 μL sample of the headspace gas was removed via gastight syringe and analyzed by gas chromatography. Using the moles of H_2 produced (0.29 mmol) and the charge passed (29.3 C), a current efficiency of 94 ± 5% was calculated for H_2 production.

X-ray Diffraction Studies. Crystals of appropriate size were mounted on a nylon fiber using NVH immersion oil, transferred to a Brüker-AXS Kappa APEX II CCD diffractometer (Mo−Kα radiation source; λ = 0.71073 Å; graphite monochromator), and cooled to the data collection temperature of 100(2) K. Unit cell parameters were obtained from 90 data frames, 0.3° Φ, from three different sections of the Ewald sphere. The raw data were integrated, and the unit cell parameters refined using SAINT. Data analysis was performed using XPREP. The data sets were treated with SADABS absorption corrections based on redundant multiscan data (Sheldrick, G,.Bruker-AXS, 2001). Structure solutions and refinements were performed using SHELXTL-97 (Sheldrick, 2008). All nonhydrogen atoms were refined with anisotropic displacement parameters. All hydrogen atoms were treated as idealized contributions. Crystal data for $[Ni(P^{Ph}{}_2N^{C6H4Me}{}_2)_2](BF_4)_2$ and $[Ni(P^{Ph}{}_2N^{C6H4OMe}{}_2)_2](BF_4)_2$ are shown in Table S3, Supporting Information.

Crystals of $[Ni(P^{Ph}{}_2N^{C6H4Me}{}_2)_2](BF_4)_2$ suitable for X-ray diffraction studies were grown from a THF/ether solution at room temperature. Preliminary data indicated a primitive monoclinic cell, and systematic absences were consistent with the space group, $P2_1/n$. The asymmetric unit contains one $[Ni(P^{Ph}{}_2N^{C6H4Me}{}_2)_2]^{2+}$ cation, two BF_4^- anions, and two molecules of THF solvent located on general positions, yielding Z = 4 and Z' = 1. One of the BF_4^- anions is disordered over two positions. These positions were located from the difference map and restrained to be equivalent using SADI and EADP commands to stabilize

the refinement. One of the molecules of THF is also disordered, but this disorder is minor and does not affect the overall identity of the structure, so it was ignored. This accounts for the 1.45 intensity Q-peak remaining in the list. The C44 methyl carbon has a larger than average ellipsoid compared to the rest of the structure. This atom is not incorrectly assigned, as the bond distances are comparable to the three other tolyl methyl bonds in the structure, and the protons for this methyl can be found in the difference map.

Crystals of $[Ni(P^{Ph}{}_2N^{C6H4OMe}{}_2)_2](BF_4)_2$ suitable for X-ray diffraction studies were grown from an acetonitrile/ether solution at room temperature. Preliminary data indicated a primitive monoclinic cell, and systematic absences were consistent with the space group, $P2_1/c$. The asymmetric unit contains one $[Ni(P^{Ph}{}_2N^{C6H4OMe}{}_2)_2]^{2+}$ cation, two BF_4^- anions, and one molecule of acetonitrile solvent located on general positions, yielding $Z = 4$ and $Z' = 1$. Although the R factor is below 10% ($R1 = 8.28\%$), the data collected were of very low intensity, as indicated by the abnormally large R(int) value and the low goodness-of-fit. However, the structure parameters, esd values, and thermal parameters are within the expected range for a structure having the given $R1$ value.

■ ASSOCIATED CONTENT

Supporting Information. Cif files for X-ray structures. Crystal data and structure refinement details. Analysis of voltammograms. Identification of maximum catalytic current (i_{cat}). Additional tabulated results for electrocatalytic hydrogen production mediated by $[Ni(P^{Ph}{}_2N^{C6H4X}{}_2)_2](BF_4)_2$ complexes. This material is available free of charge via the Internet at http://pubs.acs.org/.

■ AUTHOR INFORMATION

Corresponding Authors
john.roberts@pnl.gov, daniel.dubois@pnl.gov

■ ACKNOWLEDGMENT

We thank the reviewers for very helpful comments on the presentation of these results. This research was supported as part of the Center for Molecular Electrocatalysis, an Energy Frontier Research Center funded by the U.S. Department of Energy, Office of Science, Office of Basic Energy Sciences. Pacific Northwest National Laboratory is operated by Battelle for the U.S. Department of Energy.

■ REFERENCES

(1) (a) Fontecilla-Camps, J. C.; Volbeda, A.; Cavazza, C.; Nicolet, Y. *Chem. Rev.* **2007**, *107*, 4273–4303. (b) Peters, J. W.; Lanzilotta, W. N.; Lemon, B. J.; Seefeldt, L. C. *Science* **1998**, *282*, 1853–1858. (c) Hofacker, I.; Schulten, K. *Proteins: Struct., Funct., Genet.* **1998**, *30*, 100–107.

(2) Frey, M. *ChemBioChem* **2002**, *3*, 153–160.

(3) Nicolet, Y.; de Lacey, A. L.; Vernède, X.; Fernandez, V. M.; Hatchikian, E. C.; Fontecilla-Camps, J. C. *J. Am. Chem. Soc.* **2001**, *123*, 1596–1601.

(4) (a) Ott, S.; Kritikos, M.; Åkermark, B.; Sun, L.; Lomoth, R. *Angew. Chem., Int. Ed.* **2004**, *43*, 1006–1009. (b) Schwartz, L.; Eilers, G.; Eriksson, L.; Gogoll, A.; Lomoth, R.; Ott, S. *Chem. Commun.* **2006**, 520–522. (c) Löscher, S.; Schwartz, L.; Stein, M.; Ott, S.; Haumann, M. *Inorg. Chem.* **2007**, *46*, 11094–11105. (d) Jiang, S.; Liu, J.; Shi, Y.; Wang, Z.; Akermark, B.; Sun, L. *Dalton Trans.* **2007**, 896–902. (e) Barton, B. E.; Olsen, M. T.; Rauchfuss, T. B. *J. Am. Chem. Soc.* **2008**, *130*, 16834–16835. (f) Wang, N.; Wang, M.; Liu, J.; Jin, K.; Chen, L.; Sun, L. *Inorg. Chem.* **2009**, *48*, 11551–11558. (g) Lough, A. J.; Park, S.; Ramachandran, R.; Morris, R. H. *J. Am. Chem. Soc.* **1994**, *116*, 8356–8357. (h) Park, S.; Lough, A. J.; Morris, R. H. *Inorg. Chem.* **1996**, *35*, 3001–3006. (i) Xu, W.; Lough, A. J.; Morris, R. H. *Inorg. Chem.* **1996**, *35*, 1549–1555. (j) Lee, D.-H.; Patel, B. P.; Clot, E.; Eisenstein, O.; Crabtree, R. H. *Chem. Commun.* **1999**, 297–298. (k) Crabtree, R. H.; Siegbahn, P. E. M.; Eisenstein, O.; Rheingold, A. L.; Koetzle, T. F. *Acc. Chem. Res.* **1996**, *29*, 348–354. (l) Chu, H. S.; Lau, C. P.; Wong, K. Y.; Wong, W. T. *Organometallics* **1998**, *17*, 2768–2777. (m) Ayllon, J. A.; Sayers, S. F.; Sabo-Etienne, S.; Donnadieu, B.; Chaudret, B; Clot, E. *Organometallics* **1999**, *18*, 3981–3990. (n) Custelcean, R.; Jackson, J. E. *Chem. Rev.* **2001**, *101*, 1963–1980. (o) Shook, R. L.; Borovik, A. S. *Inorg. Chem.* **2010**, *49*, 3646–3660. (p) Yang, J. Y.; Nocera, D. G. *J. Am. Chem. Soc.* **2007**, *129*, 8192–8198. (q) Yeh, C.-Y.; C. J.; Nocera, D. G. *J. Am. Chem. Soc.* **2001**, *123*, 1513–1514.

(5) (a) Rakowski DuBois, M.; DuBois, D. L. *Chem. Soc. Rev.* **2009**, *38*, 62–72.(b) Rakowski DuBois, M.; DuBois, D. L. Chapter 7 In *Catalysis without Precious Metals*; R. M. Bullock, Ed.; , Wiley-VCH: Weinheim, Germany, 2010; pp 165−180.

(6) Rakowski DuBois, M.; DuBois, D. L. *Acc. Chem. Res.* **2009**, *42*, 1974–1982.

(7) Curtis, C. J.; Miedaner, A.; Ciancanelli, R. F.; Ellis, W. W.; Noll, B. C.; Rakowski DuBois, M.; DuBois, D. L. *Inorg. Chem.* **2003**, *42*, 216–227.

(8) Henry, R. M.; Shoemaker, R. K.; DuBois, D. L.; Rakowski DuBois, M. *J. Am. Chem. Soc.* **2006**, *128*, 3002–3010.

(9) Yang, J. Y.; Bullock, R. M.; Shaw, W. J.; Twamley, B.; Fraze, K.; Rakowski DuBois, M.; DuBois, D. L. *J. Am. Chem. Soc.* **2009**, *131*, 5935–5945.

(10) Wilson, A. D.; Newell, R. H.; McNevin, M. J.; Muckerman, J. T.; Rakowski DuBois, M.; DuBois, D. L. *J. Am. Chem. Soc.* **2006**, *128*, 358–366.

(11) Wilson, A. D.; Fraze, K.; Twamley, B.; Miller, S. M.; DuBois, D. L.; Rakowski DuBois, M. *J. Am. Chem. Soc.* **2008**, *130*, 1061–1068.

(12) Wilson, A. D.; Shoemaker, R. K.; Meidaner, A.; Muckerman, J. T.; Rakowski DuBois, M.; DuBois, D. L. *Proc. Natl. Acad. Sci U.S.A.* **2007**, *104*, 6951–6956.

(13) Jacobsen, G. M.; Yang, J. Y.; Twamley, B.; Wilson, A. D.; Bullock, R. M.; Rakowski DuBois, M.; DuBois, D. L. *Energy Environ. Sci.* **2008**, *1*, 167–174.

(14) Yang, J.; Chen, S.; Dougherty, W. G.; Kassel, W. S.; Bullock, R. M.; DuBois, D.; Raugei, S.; Rousseau, R.; Dupuis, M.; Rakowski DuBois, M. *Chem. Commun.* **2010**, *46*, 8618–8620.

(15) Wiedner, E. S.; Yang, J. Y.; Dougherty, W. G.; Kassel, W. S.; Bullock, R. M.; Rakowski DuBois, M.; DuBois, D. L. *Organometallics* **2010**, *29*, 5390–5401.

(16) Yang, J. Y.; Bullock, R. M.; Doughtery, W. G.; Kassel, W. S.; Twamley, B.; DuBois, D. L.; Rakowski DuBois, M. *Dalton Trans.* **2010**, *39*, 3001–3010.

(17) Fraze, K.; Wilson, A. D.; Appel, A. M.; Rakowski DuBois, M.; DuBois, D. L. *Organometallics* **2007**, *26*, 3918–3924.

(18) Berning, D. E.; Noll, B. C.; DuBois, D. L. *J. Am. Chem. Soc.* **1999**, *121*, 11432–11447.

(19) (a) *Elemental Radii*; Cambridge Crystallographic Data Centre: Cambridge, U.K.; http://www.ccdc.cam.ac.uk/products/csd/radii/. Accessed September 18, 2010. (b) Cordero, B.; Gómez, V.; Platero-Prats, A. E.; Revés, M.; Echeverría, J.; Cremades, E.; Barragán, F.; Alvarez, S. *Dalton Trans.* **2008**, *21*, 2832–2838.

(20) Bard, A. J.; Faulkner, L. R. *Electrochemical Methods: Fundamentals and Applications*, 2nd ed.; John Wiley & Sons: Hoboken, NJ, 2001; p 231.

(21) Kaljurand, I.; Kütt, A.; Sooväli, L.; Rodima, T.; Mäemets, V.; Leito, I.; Koppel, I. A. *J. Org. Chem.* **2005**, *70*, 1019–1028.

(22) Coetzee, J. F.; Padmanabhan, G. R. *J. Am. Chem. Soc.* **1965**, *87*, 5005–5010.

(23) Pool, D. H.; DuBois, D. L. *J. Organomet. Chem.* **2009**, *694*, 2858–2865.

(24) (a) Nicholson, R. S.; Shain, I. *Anal. Chem.* **1964**, *36*, 706–723. (b) Savéant, J. M.; Vianello, E. *Electrochim. Acta* **1965**, *10*, 905–920. (c) Savéant, J. M.; Vianello, E. *Electrochim. Acta* **1967**, *12*, 629–646.

(25) Felton, G. A. N.; Glass, R. S.; Lichtenberger, D. L.; Evans, D. H. *Inorg. Chem.* **2006**, *45*, 9181–9184.
(26) Izutsu, K. *Acid-Base Dissociation Constants in Dipolar Aprotic Solvents*. Blackwell Scientific Publications: Oxford, 1990; p 165.
(27) Kolthoff, I. M.; Chantooni, M. K., Jr.; Bhowmik, S. *Anal. Chem.* **1967**, *39*, 1627–1633.
(28) Appel, A. M.; Lee, S.-J.; Franz, J. A.; DuBois, D. L.; Rakowski DuBois, M.; Twamley, B. *Organometallics* **2009**, *28*, 749–754.
(29) (a) Munshi, P.; Main, A. D.; Linehan, J, C.; Tai, C.-C; Jessop, P. G. *J. Am. Chem. Soc.* **2002**, *124*, 7963–7971. (b) Roy, D.; Patel, C.; Sunoj, R. B. *J. Org. Chem.* **2009**, *74*, 6936–6943. (c) Matkovskii, P.; Startseva, G.; Churkina, V.; Knerel'man, E.; Davydova, G.; Vasil'eva, L.; Yarullin, R. *Polym. Sci. Series A* **2008**, *50*, 1175–1186.
(30) Chen, S.; Raugei, S.; Rousseau, R.; Dupuis, M.; Bullock, R. M. *J. Phys. Chem. A* **2010**, *114*, 12716–12724.
(31) (a) Hu, X.; Brunschwig, B. S.; Peters, J. C. *J. Am. Chem. Soc.* **2007**, *129*, 8988–8998. (b) Le Goff, A.; Artero, V.; Jousselme, B.; Tran, P. D.; Guillet, N.; Métayé1, R.; Fihri, A.; Palacin, S.; Fontecave, M. *Science* **2009**, *326*, 1384–1387. (c) Koca, A.; Özçeşmeci, M.; Hamuryudan, E. *Electroanalysis* **2010**, *22*, 1623–1633.
(32) Bernatis, P. R.; Miedaner, A.; Haltiwanger, R. C.; DuBois, D. L. *Organometallics* **1994**, *13*, 4835–4843.
(33) (a) McCrory, C. C. L.; Ottenwaelder, X.; Stack, T. D. P.; Chidsey, C. E. D. *J. Phys. Chem. A* **2007**, *111*, 12641–12650. (b) Sehlotho, N.; Nyokong, T. *J. Electroanal. Chem.* **2006**, *595*, 161–167.
(34) Berning, D. E.; Miedaner, A.; Curtis, C. J.; Noll, B. C.; Rakowski DuBois, M.; Dubois, D. L. *Organometallics* **2001**, *20*, 1832–1839.
(35) Gagliardi, L. G.; Castells, C. B.; Ràfols, C.; Rosés, M.; Bosch, E. *J. Chem. Eng. Data* **2007**, *52*, 1103–1107.
(36) (a) Rossin, A.; Gonsalvi, L.; Phillips, A. D.; Maresca, O.; Lledos, A.; Peruzzini, M. *Organometallics* **2007**, *26*, 3289–3296. (b) Friedrich, A.; Drees, M.; Schmedt auf der Gunne, J.; Schneider, S. *J. Am. Chem. Soc.* **2009**, *131*, 13584–13585. (c) Hadzovic, A.; Song, D.; MacLaughlin, C. M.; Morris, R. H. *Organometallics* **2007**, *26*, 5987–5999. (d) Casey, C. P.; Johnson, J. B.; Singer, S. W.; Cui, Q. *J. Am. Chem. Soc.* **2005**, *127*, 3100–3109.
(37) Favier, I.; Duñach, E. *Tetrahedron Lett.* **2004**, *45*, 3393–3395.
(38) Hathaway, B. J.; Holah, D. G.; Underhill, A. E. *J. Chem. Soc.* **1962**, 2444–2448.
(39) (a) Arbuzov, B. A.; Erastov, O. A.; Nikonov, G. N.; Arshinova, R. P.; Romanova, I. P.; Kadyrov, R. A. *Russ. Chem. Bull.* **1983**, *32*, 1672. (b) Maerkl, V. G.; Jin, Y. G.; Schoerner, C. *Tetrahedron Lett.* **1980**, *21*, 1409.